0026-895X/06/6904-1356–1365$20.00
MOLECULAR PHARMACOLOGY
Copyright © 2006 The American Society for Pharmacology and Experimental Therapeutics
Mol Pharmacol 69:1356–1365, 2006

Vol. 69, No. 4
17970/3094925
Printed in U.S.A.

Interaction of *d*-Tubocurarine with Potassium Channels: Molecular Modeling and Ligand Binding

Alexei Rossokhin, Georgeta Teodorescu, Stephan Grissmer, and Boris S. Zhorov

Department of Biochemistry and Biomedical Sciences, McMaster University, Hamilton, Ontario, Canada (A.R., B.S.Z.); and Department of Applied Physiology, University of Ulm, Ulm, Germany (G.T., S.G.)

Received August 10, 2005; accepted January 3, 2006

ABSTRACT

Potassium channels play fundamental roles in physiology. Chemically diverse drugs bind in the pore region of K^+ channels. Here, we homology-modeled voltage- and Ca^{2+}-gated K^+ channel BK and voltage-gated Kv1.3 using the X-ray structures of MthK and Kv1.2, respectively, and simulated the binding of *d*-tubocurarine in the inner pore of the channels. Monte Carlo minimization predicted that *d*-tubocurarine can bind in the open pore of both channels with its long axis parallel to the pore axis. The cationic groups of *d*-tubocurarine can displace K^+ from the ion dehydration site at the selectivity filter. The predicted binding energy of *d*-tubocurarine in Kv1.3 is less preferable than in BK. To test this prediction, the currents through Kv1.3 and BK channels were measured in the absence and presence of *d*-tubocurarine. Results show that *d*-tubocurarine blocks current through Kv1.3 when applied from either side of the membrane only in millimolar concentrations (K_d = 1 mM), whereas half-blocking concentrations of the internally applied *d*-tubocurarine to BK are as low as ~8 μM. This indicates that the affinities of both external and internal *d*-tubocurarine to Kv1.3 are much lower than those to BK channels. Our study reveals the K^+ dehydration site as a determinant of the *d*-tubocurarine receptor, predicts binding modes of *d*-tubocurarine in K^+ channels, and suggests that the open pore in BK is wider than in Kv1.3. The results imply that MthK can be used for homology modeling of the pore region of channels activated by forces applied to the inner helices.

K^+ channels, the most diverse group of ion channels expressed in a wide range of organisms from viruses to mammals, control the electrical activity of excitable cells (Hille, 2001). These channels play the major role in cell physiology, being involved in neuronal plasticity (Mathie et al., 1998; Hille, 2001; Birnbaum et al., 2004), salt and water exchange in epithelia, immune response, and other functions. Because of the fundamental roles of K^+ channels in physiology, their pharmacological regulation is a subject of intensive studies (Chandy et al., 2004; Tamargo et al., 2004).

The pore-forming subunit of K^+ channels consists of four domains arranged around the central pore. Each domain contains the outer and inner transmembrane helices linked at the extracellular side by the membrane-diving P-loop as well as other segments that do not contribute directly to the pore. The inner pore of the P-loop channels is a target for various drugs (for review, see Zhorov and Tikhonov, 2004). The crystal structures of prokaryotic K^+ channels KcsA (Doyle et al., 1998) and KirBac (Kuo et al., 2003) show an inverted-cone inner pore with the closed activation gate at the cone vertex and selectivity filter region at the cone base. The rather small water-lake cavity in closed channels can accommodate flexible ligands such as tetrabutylammonium (Zhou et al., 2001), which gets trapped as KcsA transits from the open to the closed state. In the closed channel, tetrabutylammonium protrudes its flexible chains in the interfaces between the four domains (Lenaeus et al., 2005). Three crystallographic structures of the open K^+ channels are available: Ca^{2+}-activated MthK (Jiang et al., 2002), voltage-gated KvAP (Jiang et al., 2003), and voltage-gated Kv1.2 (Long et al., 2005a).

Complexes of various P-loop channels with drugs can be modeled using available crystallographic structures of K^+ channels. However, the choice of templates for homology modeling remains a problem. Indeed, MthK, KvAP, and

This work was supported by a grant from the National Sciences and Engineering Research Council of Canada (to B.S.Z.) and grants from the Deutsche Forschungsgemeinschaft (Gr848/8-2) and 4SC, Martinsried (to S.G.). B.S.Z. is a recipient of the Senior Scientist award from the Canadian Institutes of Health Research. A.R. is on leave from Brain Research Institute, Moscow, Russia

Article, publication date, and citation information can be found at http://molpharm.aspetjournals.org.

doi:10.1124/mol.105.017970.

ABBREVIATIONS: BK, large conductance Ca^{2+}- and voltage-activated K^+ channel; dTC_i, intracellularly applied *d*-tubocurarine; dTC_o, extracellularly applied *d*-tubocurarine; KcsA, pH-gated K^+ channel from *Streptomyces lividans*; Kv, voltage-gated potassium channel; KvAP, voltage-dependent K^+ channel from *Aeropyrum pernix*; MCM, Monte Carlo with energy minimization; MthK, Ca^{2+}-gated K^+ channel from *Methanobacterium thermoautotrophicum.*

Kv1.2 have different geometry of the open pore. MthK is activated by forces applied to the inner helices, which are connected to the Ca^{2+}-binding cytoplasmic domains (Jiang et al., 2002). KvAP and Kv1.2 are activated by forces applied to the outer helices, which are connected to the voltage-sensing domains (Jiang et al., 2003; Long et al., 2005b). The different pore geometry may be a consequence of the different mechanisms of activation of these channels.

The pore size in ion channels can be probed by drugs whose dimensions are comparable with the pore width (Zhorov et al., 1991; Tikhonov and Zhorov, 1998). Such dimensions are characteristic of a well known curare alkaloid *d*-tubocurarine, which can be approximated by a parallelepiped of $\sim 8.5 \times 11 \times 17$ Å (Zhorov and Brovtsyna, 1993). The rib of 17 Å is larger that the width of the open pore, suggesting that it should extend along the pore axis, whereas the ribs of 8.5 and 11 Å should orient normally to the pore axis. The rib of 11 Å matches the width of the open pore in MthK, but it is larger than that in KvAP and Kv1.2. These rough estimates do not take into consideration the flexibility of *d*-tubocurarine and the channels. *d*-Tubocurarine is known to block large conductance Ca^{2+}- and voltage-activated K^+ channels (BKs) in micromolar concentrations from the cytoplasmic side (Egan et al., 1993; Baron et al., 1996). However, no data are available on *d*-tubocurarine binding to Kv channels.

In this work, we used the X-ray structures of MthK and Kv1.2 to build homology models of BK and Kv1.3, respectively. We further used the Monte Carlo with energy minimization (MCM) method to systematically search for energetically optimal binding modes of *d*-tubocurarine in BK and Kv1.3. In the predicted lowest-energy complexes, the K^+ dehydration site at the cytoplasmic side of the selectivity filter was found to be an important determinant of the *d*-tubocurarine receptor. The predicted binding energy of *d*-tubocurarine in Kv1.3 is higher (less preferable) than in BK. To verify this prediction, electrophysiological experiments were performed on the ability of *d*-tubocurarine to block current through BK and Kv1.3 channels. Therefore, we used inhibition of current by *d*-tubocurarine as an indirect measure of *d*-tubocurarine binding. We used the whole cell recording mode of the patch-clamp technique to measure current through Kv1.3 in the absence and presence of either externally or internally applied *d*-tubocurarine. In addition, we measured current through BK channels in the absence and presence of internally applied *d*-tubocurarine. Results of the experiments have confirmed the molecular modeling prediction, showing that *d*-tubocurarine can block Kv1.3, but only at millimolar concentrations. Our study proposes the binding modes of *d*-tubocurarine in K^+ channels and suggests that MthK is a reasonable template to model Ca^{2+}- and ligand-activated P-loop channels.

Materials and Methods

Molecular Modeling. The X-ray structure of MthK was used as a template to build the homology model of BK. The Kv1.3 channel was modeled using Kv1.2 as a template. The models contain four domains, each domain comprising two transmembrane segments, S5 and S6, and a membrane-diving P-loop. Amino acid sequences are aligned as shown in Table 1. Residues are designated using the nomenclature proposed for P-loop channels (Zhorov and Tikhonov, 2004), with a superscript label that contains the segment identification (p, P-loop; i, inner helix) and the relative number of residue in the alignment with the corresponding segment of KcsA. For example, Thr75 in the selectivity filter of KcsA is designated Thr^{p49} (Table 1).

Starting values for backbone torsions in the models were taken from the template. The side chain torsions in those residues, which were identical in a template and corresponding model, were assigned starting values as in the template. All-*trans* starting conformations were assigned to side chains of other residues.

The conformational energy expression included van der Waals, electrostatic, hydration, and torsion components. Bond angles of the protein were fixed. Bond angles of *d*-tubocurarine were varied, and energy of their deformation contributed to the conformational energy. The hydration energy was calculated by the implicit-solvent method (Lazaridis and Karplus, 1999). Electrostatic interactions were calculated with a distant-dependent dielectric ($\epsilon = r$). Nonbonded interactions were calculated using the AMBER force field (Weiner et al., 1984) with a cut-off distance of 9 Å. Electrostatic interactions involving ionized groups were calculated without a cut-off.

The MCM method (Li and Scheraga, 1987) was applied to find the lowest energy conformations of the channels, *d*-tubocurarine, and their complexes. Energy was minimized in the space of generalized coordinates using the ZMM program (http://www.zmmsoft.com). The atomic charges of *d*-tubocurarine were calculated by the AM1 method (Dewar et al., 1985) using the MOPAC program. The geometry of *d*-tubocurarine was optimized using an HGRID (Hot GRID) procedure that submits a large number of MCM trajectories from randomly generated starting points and collects low-energy structures found in each trajectory.

The channel models were optimized by the two-stage MCM protocol. In the first MCM stage, the backbone geometry was kept fixed, whereas side chains were allowed to move. This trajectory relaxed bad contacts that emerged in the first stage of homology modeling. The optimal structure obtained in the first MCM trajectory was used

TABLE 1

Aligned sequences of K^+ channels

Residues that contribute to *d*-tubocurarine binding in the models of BK and Kv1.3 are underlined. Bold type indicates residues in which mutation affects binding of ligands in Kv1.3 (Hanner et al., 2001), HERG (Mitcheson et al., 2000), Kv1.5 (Decher et al., 2004), and Kv7.1 (Seebohm et al., 2003).

	P-loop			Inner helix			
	33	41	51[a]	1	11	21	31[a]
KcsA	LITYPRAL	WWSVETATTV	GYGD	LWGRLVAVVV	MVAGITSFGL	VTAALATWFV	G
MthK	GESWTVSL	YWTFVTIATV	GYGD	PLGMYFTVTL	IVLGIGTFAV	AVERLLEFLI	N
KvAP	IKSVFDAL	WWAVVTATTV	GYGD	PIGKVIGIAV	MLTGISALTL	LIGTVSNMFQ	K
BK	ALTYWECV	YLLMVTMSTV	GYGD	TLGRLFMVFF	ILGGLAMFAS	YVPEIIELIG	N
SK3				YCGKGVCLLT	GIMGAGCTAL	VVAVVARKLE	L
Kv1.3	FNSIPDAF	WWAVVTMTTV	GYGD	IGGKIVGSLC	**A**IAG**VLT**I**AL**	**PVP**VIVSNFN	Y
Kv1.5	FSSIPDAF	WWAVVTM**TT**V	GYGD	VGGKIVGSLC	AIAGVLTIAL	P**V**PVI**V**SNFN	Y
HERG	KDKYVTAL	YFTFSSL**TSV**	GFGN	NSEKIFSICV	MLIGSLMYAS	I**F**GN**V**SAIIQ	R
Kv7.1	FGSYADAL	WWGVVT**V**T**T**I	GYGD	WVGKTIASCF	SVF**AI**S**FFA**L	P**A**GILGSGFA	L

HERG, human *ether-a-go-go*-related gene.

[a] Relative numbers of residues (Zhorov and Tikhonov, 2004).

as the starting point for the second MCM trajectory, in which both the backbone and side chains were relaxed. Each MCM trajectory was terminated when the last 2000 consecutive energy minimizations did not improve the energy. Pin constraints between matching α-carbons in the model and in the X-ray structure were used to prevent large deviations between the model and the template. The pins were defined by a flat-bottom parabolic penalty function (Brooks et al., 1985) that increases with the deviation of an α-carbon atom from the template position.

The homology models of BK and Kv1.3 were used to dock *d*-tubocurarine. The optimal complexes between *d*-tubocurarine and the channel proteins were searched by sampling positions, orientations, and torsion angles of the ligand as well as torsion angles of the protein side chains. The energy of each sampled structure was Monte Carlo-minimized in the space of all generalized coordinates, including the protein backbone torsion and bond angles of the ligand. The MCM protocol eliminates bad contacts and predicts an energetically optimal structure in a certain area around the starting point. The dimensions of the area increase but slowly with the length of the MCM trajectory. Therefore, the probability to find the energetically best geometry of the ligand-channel complex for an arbitrary placed *d*-tubocurarine is low. To address this problem, we searched the lowest energy complexes systematically by taking advantage of the fact that *d*-tubocurarine has the shape of a flattened ellipsoid. The length of *d*-tubocurarine between most distant atoms at the poles is larger than the width of the open pore in both the MthK- and Kv1.2-based models. This rules out *d*-tubocurarine binding with the long axis perpendicular to the pore axis. Two binding modes of *d*-tubocurarine with its long axis collinear to the pore axis are possible, with either the quaternary ammonium or protonated amino group facing the selectivity filter. In both of the modes, the *d*-tubocurarine shape is approximately complementarily to the pore region of the open channel. The starting positions of *d*-tubocurarine in the channel were sampled systematically in the space of the essential (driven) generalized coordinate, which specifies rotation of *d*-tubocurarine around its long axis. Other generalized coordinates, which include five remaining rigid-body degrees of freedom of *d*-tubocurarine, torsional angles of *d*-tubocurarine and channel, and bond angles of *d*-tubocurarine were Monte Carlo-minimized for each value of the essential generalized coordinate. The values of ligand-receptor energy extracted from the energetically best structure found from each starting orientation were plotted against the driven generalized coordinate as described previously (Tikhonov and Zhorov, 2005).

Cells. The L929 cells, permanently transfected with mKv1.3 (Grissmer et al., 1994), were maintained in Dulbecco's modified Eagle's medium with Earle's salts (catalog no. 41966-029; Invitrogen, Paisley, UK) and 10% heat-inactivated fetal calf serum (Invitrogen, Karlsruhe, Germany). The CHO-K1 cells, permanently transfected with the BK or MaxiK channel α-hslo together with the β-bslo (GenBank accession no. L26101) subunit (Zhou et al., 1998), were kindly provided by Dr. P. Ruth (Department of Pharmacology and Toxicology, Technical University Munich, Munich, Germany). The cells were maintained in the same culture medium used for L929 cells, supplemented with 10% heat-inactivated fetal calf serum, 250 μg/ml G418 (Geneticin), 100 μg/ml hygromycin B, 10 ml of HT-Supplement (0.68 g/l hypoxanthine and 0.194 g/l thymidine), 5 ml of nonessential amino acids (without L-Gln, 1.15 mg/ml L-Pro). These culture medium supplements were purchased from Invitrogen, and the cell culture materials were from Dow Corning (Seneffe, Belgium). Cells were kept in a humidified 10 or 5% CO_2 incubator (Kendro Laboratory Products GmbH, Hanau, Germany) at 37°C.

Solutions. All experiments were carried out at room temperature (21–25°C). Cells were measured in normal mammalian Ringer's solution containing, for Na^+ Ringer, 160 mM NaCl, 4.5 mM KCl, 2 mM $CaCl_2$, 1 mM $MgCl_2$, and 5 mM HEPES, and for K^+ Ringer, NaCl was replaced by KCl (final $[K^+]$ 164.5 mM). The pH was adjusted to 7.4 with NaOH and KOH, respectively, with an osmolarity from 290 to 320 mOsM. A simple syringe-driven perfusion system was used to exchange the bath solution in the recording chamber. The internal pipette solution used for measuring Kv1.3 currents contained 155 mM KF, 2 mM $MgCl_2$, 10 mM EGTA, and 10 mM HEPES; the solution used for measuring current through Ca^{2+}-activated potassium channels (BK or MaxiK) contained 135 mM potassium aspartate, 8.7 mM $CaCl_2$, 2 mM $MgCl_2$, 10 mM EGTA, and 10 mM HEPES (free $[Ca^{2+}]_i = 10^{-6}$ M). The pH was adjusted to 7.2 with KOH in each solution, and each had an osmolarity between 290 and 320 mOsM. All chemicals of quality "pro analysis" were obtained from the following companies: Fluka Chemika GmbH (Neu-Ulm, Germany) (HEPES), Carl-Roth Chemika GmbH+Co. (Karlsruhe, Germany) ($CaCl_2$), Merck KGaA (Darmstadt, Germany) (NaCl), Sigma-Aldrich Chemie GmbH (Steinheim, Germany) (EGTA), and Fluka Chemika GmbH (Buchs, Germany) (KCl, KF, and $MgCl_2$). *d*-Tubocurarine was purchased through Fluka BioChemika GmbH (Buchs, Germany), dissolved under argon conditions in water (stock solution of 64 mM), and diluted to the final concentrations in the bath solution for external application and in the pipette solution for internal application of *d*-tubocurarine. For internal application of *d*-tubocurarine, the pipette was first tip-filled with *d*-tubocurarine-free internal solution by dipping the pipette tip into the internal solution and applying suction to the pipette. Then, the internal solution with the different *d*-tubocurarine concentrations was used to fill the remainder of the patch pipette from the back.

Electrophysiology. All electrophysiological experiments were carried out using the whole cell mode of the patch-clamp technique (Hamill et al., 1981; Rauer and Grissmer, 1996). Electrodes were pulled from glass capillaries (Science Products, Hofheim, Germany) in three stages and fire-polished to resistances measured in the bath from 2.5 to 5 MΩ. Membrane currents were measured with an EPC-9 patch-clamp amplifier (HEKA Elektronik, Lambrecht/Pfalz, Germany) interfaced to a Macintosh computer running the acquisition and analysis software Pulse and PulseFit (HEKA Elektronik). The holding potential in all experiments was −80 mV. Series resistance compensation (80%) was used when currents were bigger than 2 nA. Data analysis was performed using IgorPro 3.1 (Wavemetrics, Lake Oswego, OR).

Results

Conformational Analysis of *d*-Tubocurarine. The global-minimum conformation of *d*-tubocurarine found by the HGRID procedure (Fig. 1B) is practically identical to the X-ray structure by Reynolds and Palmer (1976). This conformation has a shape of a flattened ellipsoid with the charged groups at the poles. The ellipsoid's surface between the poles has a predominantly hydrophobic character. The second-best conformation of *d*-tubocurarine (Fig. 1C) corresponds to the significantly different X-ray structure (Codding and James, 1973). The energy of this conformation is ~0.5 kcal/mol above the global minimum. The results of the brute-force global minimization are close to those reported by Zhorov and Brovtsyna (1993), despite that the latter study was performed with a different force field and a more sophisticated but laborious algorithm of conformational search (Go and Scheraga, 1970), which was the only choice at slow computers. Furthermore, we used the global-minimum conformation as a starting structure, because its ellipsoidal shape is more complementary to the cylindrical open pore than another conformation, which has a pyramidal shape (Fig. 1C).

Selectivity Filter Occupancy. Cationic ligands can approach the selectivity filter region from the cytoplasmic side, as seen in the X-ray structures of tetrabutylammonium with KcsA (Zhou et al., 2001; Lenaeus et al., 2005). The electro-

static component of the ligand-receptor energy should depend on the occupation of K^+ binding sites in the selectivity filter. The available X-ray structures of K^+ channels show different numbers of potassium ions in the selectivity filter. Two potassium ions are seen in the KcsA-antibody complex at low K^+ concentration (Zhou et al., 2001b), three in KcsA (Doyle et al., 1998), and four in KvAP (Jiang et al., 2003) as well as in the KcsA-antibody complex at high K^+ concentration (Zhou et al., 2001b) and in KcsA-tetrabutylammonium complex (Zhou et al., 2001a). Following Zhou and MacKinnon (2003), we label K^+ binding sites 1 through 4 starting from the most extracellular site. Analysis of the electron-density profiles of K^+ and Tl^+ in KcsA revealed that the four sites are occupied by potassium ions with nearly equal probability, but they bind simultaneously only two potassium ions in positions 1 and 3 or 2 and 4 (Zhou and MacKinnon, 2003). Our MCM calculations demonstrated that the selectivity filter does not hold simultaneously four potassium ions. Electrostatic repulsion displaced K^+ from position 1 in the open Kv1.3 and from position 4 in the closed Kv1.3 (data not shown). To explore various possibilities, we modeled K^+ channels with two patterns of the selectivity filter occupancy. In the first pattern, three potassium ions occupied positions 1, 3, and 4 as seen in the KcsA structure (Doyle et al., 1998). The second pattern had two potassium ions that occupied positions 1 and 3. Configuration 2, 4 was not considered, because in terms of interactions with *d*-tubocurarine it is similar to configuration 1, 3, 4.

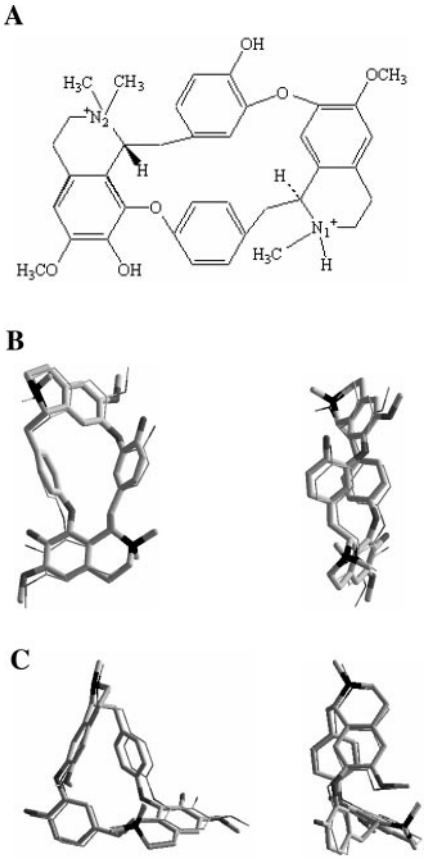

Fig. 1. Structure of *d*-tubocurarine. A, chemical formula. B and C, orthogonal views at the superposition of the X-ray structure (wire-frames) and structures predicted by the ZMM module HGRID (sticks). The global-minimum conformation (B) matches the X-ray structure by Reynolds and Palmer (1976). The second-best conformation (C) with the energy 0.5 kcal/mol above the global-minimum matches the X-ray structure by Codding and James (1973). Nitrogens and oxygens are darker than carbons.

Geometry of Threonine Rings. The inner pore of Kv1.3 has a predominantly hydrophobic character, which would favorably interact with the hydrophobic moieties of ligands. The only polar residues that could form direct contact with the ammonium groups of *d*-tubocurarine are Thr^{p48} and Thr^{p49}. Side chains of these residues adopt various orientations in different crystals (Fig. 2, A–C). Experimental values of Thr^{p49} side chain torsion χ_1 are $-32.7°$ in KcsA, 62° in KcsA-tetrabutylammonium complex, 89.5° in KvAP, and 65.7° in Kv1.2. Conformational transitions in the selectivity filter region may underline the channel transition from a conducting to a nonconducting state (Yellen, 2001; Zhou et al., 2001b; Zhou and MacKinnon, 2003). To systematically explore conformational possibilities of the Thr rings, we created a model of the Kv1.3 selectivity filter involving four decapeptides with residues p44 through p53. The α-carbons were constrained to coordinates of Kv1.2, and positions 1, 3, and 4 were populated by potassium ions. The energy was Monte Carlo-minimized from 200 starting points, in which random values of χ_1 and χ_2 were assigned to side chain torsion of Thr^{p49}.

The apparent global minimum (Fig. 2D) corresponds to the conformation seen in the X-ray structure of Kv1.2. It is stabilized by the inter-residue H^+ bonds Thr^{p49}_OH···O=C^{α}_Thr^{p48} with eight oxygens of Thr^{p49} coordinating K^+ in position 4. The average value of χ_1 in Thr^{p49} in the four domains is 81.9 ± 2.5°, which is close to the value in the

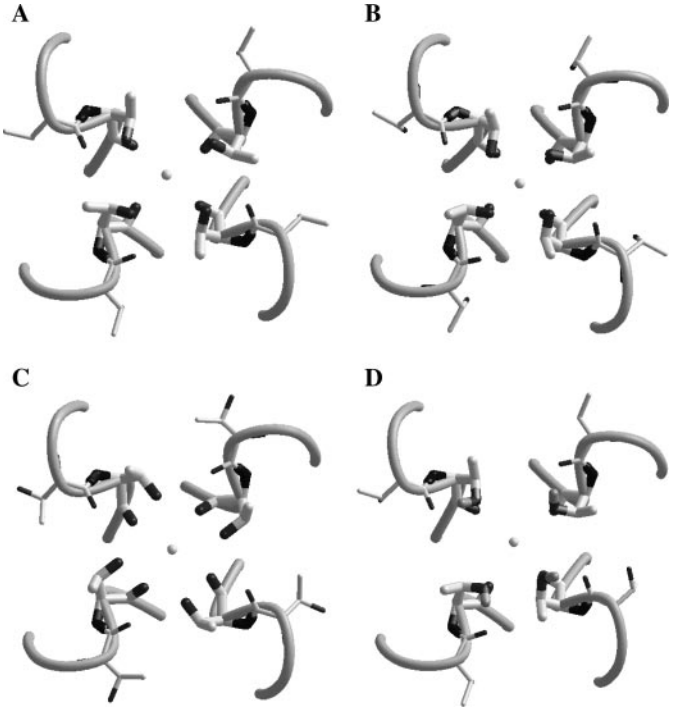

Fig. 2. Cytoplasmic views at the experimental (A–C) and predicted (D) conformations of residues Thr^{p48} and Thr^{p49} shown as thin and thick sticks, respectively. Oxygen and nitrogen atoms are darker than carbons. Rods are drawn via C^{α} atoms in positions p46 to p51. The K^+ ion in position 4 is shown as a small sphere. A, X-ray structure of Kv1.2 (Long et al., 2005a). B, X-ray structure of KvAP (Jiang et al., 2003). C, X-ray structure of KcsA (Doyle et al., 1998). D, global-minimum conformation obtained in Monte Carlo minimization of the selectivity filter model of Kv1.3.

X-ray structure of KvAP. A large number of conformations within 7 kcal/mol from the apparent global minimum were found. In some higher energy asymmetric structures, side chains of Thr^{p48} and Thr^{p49} are involved in inter- and intra-residue H-bonds. These calculations demonstrate the flexibility of Thr ring. The global-minimum conformation, which corresponds to the open channel, was chosen as the starting point for docking the open-channel blocker *d*-tubocurarine.

Docking *d*-Tubocurarine in BK and Kv1.3. To find the lowest-energy ligand-channel complexes, we first manually placed *d*-tubocurarine in BK with either the quaternary ammonium group or protonated amino group approaching the selectivity filter. Monte Carlo-minimized structures with potassium ions in positions 1 and 3 of the selectivity filter had lower ligand-receptor energy (Table 2) and were used for the systematic search of the energetically optimal ligand-receptor complexes by rotating *d*-tubocurarine in the channel. Taking into account the 4-fold symmetry of the channel, the imposed rotation angle was varied from 0 to 90° with the step of 15° (Fig. 3). At each step, the energy was Monte Carlo-minimized.

The ligand-protein energy and its components extracted from the Monte Carlo-minimized structures of *d*-tubocurarine in BK with potassium ions in positions 1 and 3 are shown in Fig. 4. In both binding modes, van der Waals energy varies from −13 to −22 kcal/mol, indicating that overlaps between the ligand and receptor atoms are eliminated by the MCM protocol at each orientation of the ligand. Electrostatic energy varies from −8 to −17 kcal/mol with major contributions from the attraction of the ligand cationic groups to Ser^{p48} and Thr^{p49}. The stabilizing van der Waals and electrostatic contributions to the ligand-protein energy are partially compensated by the destabilizing hydration energy. The hydration energy has two types of components: preferable dehydration of hydrophobic groups and nonpreferable dehydration of hydrophilic groups. The latter components prevail resulting in positive (repulsing) hydration energy observed at each orientation of the ligand.

The binding mode of *d*-tubocurarine with the protonated amino group toward the selectivity filter is more energetically preferable because of stronger van der Waals interactions and lower hydration energy (Table 3). The average distance between the amino group and $O^{\gamma}\_Thr^{p49}$ is 4.4 Å. Another factor stabilizing the complexes is the proximity of the cationic groups of *d*-tubocurarine to the focus of macrodipoles of the P-loop helices (Fig. 5, A and B).

Residues Leu^{i15}, Phe^{i18}, and Ala^{i19} provide the largest contributions to the van der Waals energy of the *d*-tubocurarine-channel complex (Table 3). The lowest energy conformation of *d*-tubocurarine can be approximated by a parallelepiped of ~8.5 × 11 × 17 Å (Zhorov and Brovtsyna, 1993). Let us designate *a*, *b*, and *c* the parallelepiped faces with dimensions of 11 × 17, 8.5 × 17, and 8.5 × 11 Å, respectively. The cationic groups of *d*-tubocurarine are at the smallest faces *c*. Four residues Phe^{i18} at the narrowest level of the pore embrace *d*-tubocurarine, but they differently interact with

TABLE 2
Lowest-energy complexes of *d*-tubocurarine in BK found by Monte Carlo-minimizing the starting conformations with manually placed ligand

Energy	Amino Group of the Ligand Approaching the Selectivity Filter and Positions Occupied by K^+ Ions			
	Tertiary		Quaternary	
	1, 3, 4	1, 3	1, 3, 4	1, 3
van der Waals, kcal/mol	−18.9	−18.0	−10.7	−14.7
Electrostatic, kcal/mol	4.6	−11.1	0.4	−4.9
Solvation, kcal/mol	10.1	11.2	3.4	5.4
Total, kcal/mol	−4.2	−17.9	−6.9	−14.2

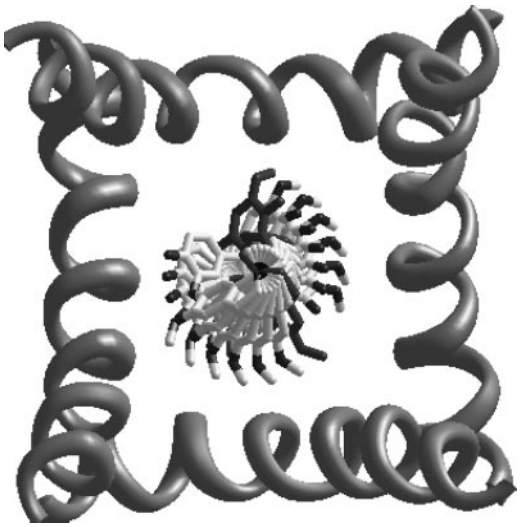

Fig. 3. The extracellular view at the superposition of starting orientations of *d*-tubocurarine in BK. The ligand is docked with the protonated amino group toward the selectivity filter. The energy of interaction of *d*-tubocurarine with BK obtained after Monte Carlo minimization of these starting orientations is shown in Fig. 4. Only inner helices of the channel are shown for clarity. The rotational angle of *d*-tubocurarine in BK is a dihedral angle between two planes. The first plane passes through the pore axis and main chain oxygen O_Thr^{p49}. The second plane passes through *d*-tubocurarine long axis and the oxygen atom bridging two phenyl rings. The dihedral angle was varied clockwise as viewed from the extracellular space with a step of 15°. *d*-Tubocurarine at the rotation angle of 0° is colored black.

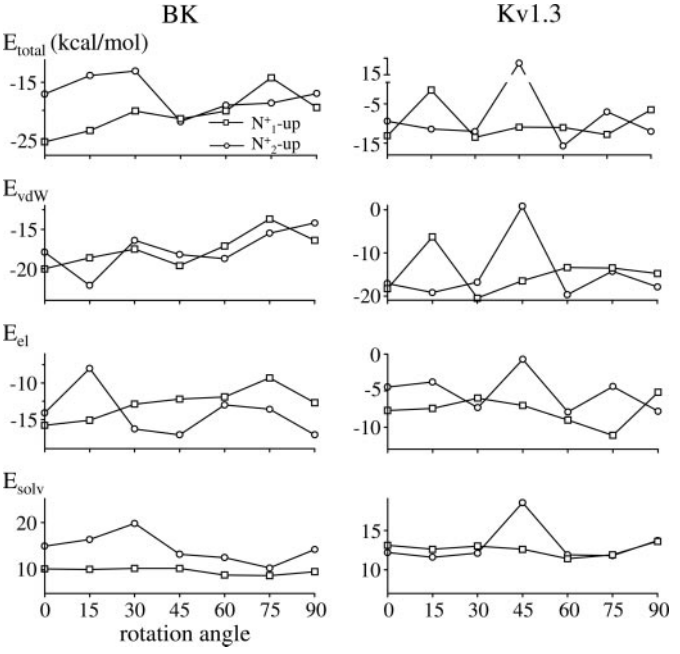

Fig. 4. *d*-Tubocurarine-channel energy (E_{total}) and its van der Waals, electrostatic, and solvation energy components against rotation angle of the ligand in the pore of BK and Kv1.3 channels.

it (Fig. 5C). Two of them protrude inside the pore to form stabilizing contacts with faces *a* that are ~8.5 Å apart. The ligand faces *b*, which are ~11 Å apart, push the other two residues Phe^{i18} against the inner helices' backbones (Fig. 5C).

Monte Carlo-minimized complexes of *d*-tubocurarine in BK with three potassium ions in the selectivity filter are less stable than complexes in the model with two potassium ions (Table 2). The former are destabilized by the stronger repulsion between the ligand's cationic group and K^+ in position 4, especially in the binding mode with the protonated amino group toward the selectivity filter. In the crystal structures of KcsA with tetrabutylammonium, the ligand's nitrogen is ~5 Å from K^+ in position 4. The electrostatic repulsion unavoidable in such a complex is compensated by four butyl groups of tetrabutylammonium, which provide multiple van der Waals contacts with the bottom of the selectivity filter region and fit into interdomain cavities (Leneaus et al., 2005). In the *d*-tubocurarine-BK complexes, the electrostatic repulsion between the ligand and K^+ in position 4 is not compensated, because face *c* of *d*-tubocurarine, which is exposed to the selectivity filter, makes less van der Waals contacts with the channel than tetrabutylammonium. Furthermore, MOPAC calculations show that the positive charge in tetrabutylammonium is completely delocalized over alkyl groups adjacent to the nitrogen atom, weakening the electrostatic repulsion from the potassium ion in position 4. Delocalization of positive charges is also seen in *d*-tubocurarine, but a charge of 0.27 proton charge units remains at the NH bond of the protonated amino group of the drug. This charge would repel K^+ in position 4.

TABLE 3

Lowest energy complexes of *d*-tubocurarine with BK channel with K^+ ions in positions 1, 3 and residues providing the largest contribution to the ligand-receptor energy

Two figures delimited by slash (/) refer to the matching residues in the four domains that provide the energy contributions of the highest and the lowest absolute values. Close numbers indicate that *d*-tubocurarine interacts with matching residues in all four domains (e.g., Thr^{p49}).

	Amino Group of the Ligand Approaching the Selectivity Filter	
	Tertiary	Quaternary
Energy		
van der Waals, kcal/mol	−20.0	−18.2
Electrostatic, kcal/mol	−15.8	−17.1
Hydration, kcal/mol	10.2	13.3
Total, kcal/mol	−25.6	−22.0
Residues		
Ser^{p48}	−2.1/−0.5	−2.2/−0.8
Thr^{p49}	−2.9/−2.0	−3.3/−2.1
Leu^{i15}	−1.2/−0.3	−1.0/0.4
Phe^{i18}	−3.2/0.4	−0.3/0.2
Ala^{i19}	−1.1/0.3	−0.8/−0.5
Val^{i22}	−0.8/0.3	0.7/−0.4

The search for the energetically optimal orientation of *d*-tubocurarine in the Kv1.2-based model of Kv1.3 predicts that orientations with either the tertiary or quaternary ammonium group toward the selectivity are possible (Fig. 6). The lowest energy complex has the ligand-receptor energy of −15.7 kcal/mol, which is ~10 kcal/mol higher than that in the MthK-based model of BK channel (Fig. 4; Table 4). The major difference in ligand-receptor energy is in electrostatic interactions, which are weaker in Kv1.3 than in BK. The electrostatic ligand-receptor interactions in Kv1.3 are desta-

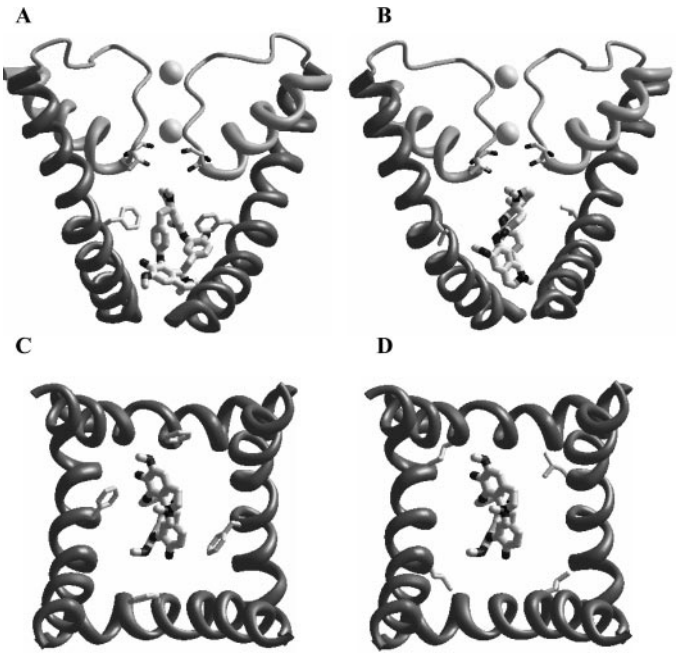

Fig. 5. Side (A and B) and extracellular (C and D) views at the lowest energy complexes of *d*-tubocurarine in BK with the protonated amino group of the ligand oriented toward (A and C) and away (B and D) from the selectivity filter with K^+ ions in positions 1 and 3. In the side views, only the inner helices and P-loops in two domains are shown for clarity. In the extracellular views, only inner helices are shown. Residues providing strong contributions to interaction with *d*-tubocurarine are shown as sticks: Thr^{p49} (A and B), Phe^{i18} (A and C), and Leu^{i15} (B and D). K^+ ions are shown as spheres.

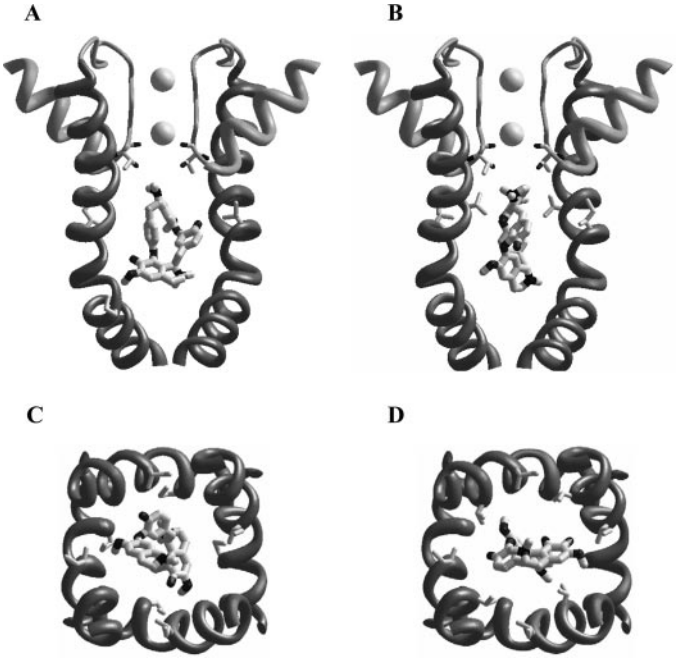

Fig. 6. Side (A and B) and extracellular (C and D) views at the lowest energy complexes of *d*-tubocurarine in Kv1.2-based model of Kv1.3 with the protonated amino group of the ligand oriented toward (A and C) and away (B and D) from the selectivity filter with K^+ ions in positions 1 and 3. The following residues providing strong contributions to interaction with *d*-tubocurarine are shown as sticks: Thr^{p49} (A and B), Pro^{i23} (A and C), and Val^{i15} (B and D). Side chains of Ile^{i18}, which are homologous to Phe^{i18} in BK, are also shown by sticks in A to D. K^+ ions are shown as spheres.

bilized by a weaker attraction of the *d*-tubocurarine cationic groups to Thr^{p49} and Thr^{p48} and a stronger repulsion of the groups from K^+ in position 3.

Ligand-Binding Experiments. To experimentally test the predicted low affinity of *d*-tubocurarine in Kv1.3, we performed whole cell patch-clamp experiments on L929 cells permanently transfected with mKv1.3. First, we wanted to see what affinity *d*-tubocurarine has to Kv1.3 when applied from the outside (dTC_o). Currents through mKv1.3 channels were elicited by stepping the voltage from a holding potential of −80 to +40 mV for 50 ms as shown in Fig. 7A. The bath solution contained 4.5 mM K^+ without (control) and with 1 μM, 100 μM, 1 mM, and 3 mM dTC_o; therefore, no tail currents could be observed.

As can be seen on Fig. 7A, currents through Kv1.3 channels were hardly affected by 1 or 100 μM dTC_o. The block only became significant at concentrations around 1 mM dTC_o or higher. From these and similar experiments, we constructed dose-response-relationships of dTC_o to block current through Kv1.3 as can be seen in Fig. 7B. The results clearly show that dTC_o can block Kv1.3, but significant block is observed only in millimolar concentrations.

In further experiments, we evaluated the affinity of *d*-tubocurarine on Kv1.3 when applied from the intracellular side (dTC_i). Because *d*-tubocurarine is only back-filled in the patch pipette and at the tip of the pipette is a *d*-tubocurarine-free internal solution, the current measurements in whole cell recording right after break-in reflect the control current without *d*-tubocurarine. During the course of each experiment, *d*-tubocurarine from the pipette will diffuse into the cell, and, because of the large volume of the back-filled solution compared with the tip-filled solution, *d*-tubocurarine will approximately reach the concentration in the back-filled solution. Currents through mKv1.3 channels were elicited by stepping the voltage from a holding potential of −80 to +40 mV for 50 ms as shown in Fig. 8A. The bath solution contained 164.5 mM K^+ to be comparable with the experiments on BK channels (Egan et al., 1993); therefore, inward tail currents could be observed in contrast to the experiments shown in Fig. 7. Different experiments with different dTC_i concentrations in the pipette are superimposed and scaled to normalize the control current.

As can be seen in Fig. 8A, current through Kv1.3 channels were little affected by 100 μM dTC_i with 1 mM dTC_i blocking about 50% of the current through Kv1.3 under our measuring conditions. The results clearly show that dTC_i cannot block Kv1.3 at concentrations below 100 μM. The affinity of dTC_i for Kv1.3 is therefore much weaker than for BK channels (Fig. 8, C and D) with concentrations of ~8 μM that reduce current by half. This affinity of dTC_i for the BK channel is similar to values obtained from the literature (Egan et al., 1993). The experiments by Egan et al. (1993) on the block of BK channels by dTC_i were performed on inside-out membrane patches of cultured olfactory bulb neurons. Single BK channels were exposed to different concentrations of *d*-tubocurarine to the internal membrane surface of an inside-out membrane patch containing a single BK channel with symmetrical 150 mM K^+ on both sides of the membrane. Application of 10 μM *d*-tubocurarine reduced the overall open time in those recordings by approximately 50% without changing the single channel conductance. Our whole cell experiments with BK as well as Kv1.3 channels are comparable with those of Egan et al. (1993) because the experiments with dTC_i on Kv1.3 were also performed in symmetrical K^+ solutions. Thus, experiments confirm the prediction of the molecular modeling that the internally applied *d*-tubocurarine has lower affinity in Kv1.3 than in BK.

TABLE 4

Interaction energy (kilocalories per mole) of *d*-tubocurarine with Kv1.2-based model of Kv1.3 with K^+ ions in positions 1, 3 and residues providing the largest contribution to the ligand-receptor energy

Two figures delimited by slash refer (/) to the matching residues in the four domains that provide the energy contributions of the highest and lowest absolute values. Close numbers indicate that *d*-tubocurarine interacts with matching residues in all four domains (e.g., Thr^{p49}).

	Cationic Group of the Ligand Approaching the Selectivity Filter with Two Potassium Ions	
	Tertiary	Quaternary
Energy		
van der Waals	−20.5	−19.7
Electrostatic	−6.0	−7.9
Hydration	13.0	11.9
Total	−13.5	−15.7
Residues		
Thr^{p48}	−1.1/0.2	−1.1/−0.6
Thr^{p49}	−2.0/−1.1	−2.5/−1.0
Val^{i15}	−1.3/0.8	−2.2/−0.3
Ile^{i18}	0.8/−0.2	−0.7/[a]
Ala^{i19}	0.8/−0.5	−1.4/0.6
Leu^{i20}	−0.9/[a]	−1.4/[a]
Val^{i22}	−0.5/0.2	0.9/0.4
Pro^{i23}	−1.8/−0.3	−1.2/−0.3

[a] Absolute value of the lowest energy contribution is less than 0.1 kcal/mol.

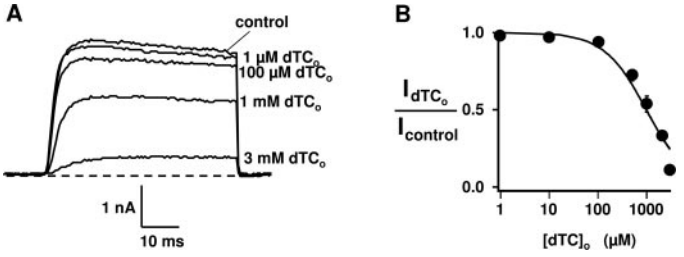

Fig. 7. Whole cell patch-clamp experiments on L929 cells permanently transfected with mKv1.3. A, currents through mKv1.3 channels were elicited by stepping the voltage to +40 mV for 50 ms from a holding potential of −80 mV every 30 s. The bath solution contained 4.5 mM K^+ without (control) and with 1 μM, 100 μM, 1 mM, and 3 mM dTC_o. B, dose-response curve for dTC_o blocking current through Kv1.3 channels. The K_d value (1 ± 0.1 mM) for the dTC_o block was deduced by fitting a modified Hill equation ($I_{dTCo}/I_{control} = 1/[1 + ([dTC_o]/K_d)]$) to the data points, where I_{dTCo} is the peak current in the presence of dTC_o and $I_{control}$ is the peak current in the absence of dTC_o. The value at each dTC_o concentration was the mean ± S.D. of six measurements. SD is shown as bars when it exceeds the size of the symbol.

Discussion

Various ligands, from simple tetraethylammonium to large alkaloids such as *d*-tubocurarine and correolide, a naturally occurring steroidal ligand with immunosuppressant activity (Hanner et al., 1999, 2001), are known to block the inner pore of K^+ channels. Molecular modeling becomes an increasingly popular approach to predict drug-channel complexes. However, the reliability of predictions, which can be made with the help of homology models, is highly sensitive to the choice of the X-ray templates. The X-ray structures for only three open K^+ channels are currently available: MthK, KvAP, and Kv1.2. It remains unclear which of the templates should be

used to model complexes of medicinally important drugs with specific K^+ channels. In this study, we have built homology models of BK and Kv1.3 channels using MthK and Kv1.2, respectively, and docked *d*-tubocurarine in the open inner pore of these channels. The approximate shape complementarity with the open inner pore predetermined the orientation of the ellipsoid-like, semirigid *d*-tubocurarine, in which the ligand's long axis is approximately collinear to the pore axis. We found that the open pore of both channels is wide enough to accommodate the drug. The binding mode with the protonated amino group toward the selectivity filter was found more preferable than the opposite mode with the quaternary ammonium group toward the selectivity filter.

To explore systematically possible orientations of *d*-tubocurarine in BK and Kv1.3 channels, we computed profiles of Monte Carlo-minimized energy against rotation of the ligand around its long axis (Fig. 4). The obtained smooth profiles of ligand-receptor energy with a shallow minimum are in a sharp contrast with the bumpy rotational profiles of tetrodotoxin and saxitoxin in the selectivity filter of the Na^+ channel, which have deep minima (Tikhonov and Zhorov, 2005). The latter complexes are stabilized by multiple H^+ bonds, whose elimination upon turning the ligand out of the most preferable orientation results in a sharp energy increase. In contrast, no H-bonds are formed in the *d*-tubocurarine-channel complexes. These are stabilized by van der Waals and electrostatic interactions, which have relatively low sensitivity to the ligand orientation. This observation can explain the fact that many structurally various ligands bind in the inner pore of K^+ channels, whereas the selectivity filter region of Na^+ channel is blocked by highly specific toxins.

Many eukaryotic voltage-gated potassium channels, including the best-studied *Shaker* channels, contain a conserved Pro-Val-Pro motif in the inner helices. Based on their studies of Cd^{2+} action on the *Shaker* channel mutants, Webster et al. (2004) derived valuable distance constraints between the inner helix residues in positions i22, i24, and i34. Bruhova and Zhorov (2005) used these distance constraints to build the KvAP-based model of the *Shaker* channel, which predicted a smooth bend at the Pro-Val-Pro motif and the pore width of ~10 Å. The predicted characteristics are consistent with the later published structure of Kv1.2 (Long et al., 2005a). The model of Bruhova and Zhorov (2005) also explained the paraxial fact that large correolide and small Cd^{2+} ions block the inner vestibule of the open Kv1.3 at the same level of the pore. The MthK-based model of the *Shaker* channel was found inconsistent with the distance constraints of Webster et al. (2004). However, this does not rule out the applicability of the MthK structure to model Ca^{2+}-activated K^+ channels as well as certain ligand-gated channels. Indeed, calculations of the current study demonstrated that *d*-tubocurarine have a higher affinity in the MthK-based model of BK than to the Kv1.2-based model of Kv1.3. The computed differences in the binding energy are determined by geometric peculiarities of the open channels rather than the different nature of the pore-facing residues. The prediction that *d*-tubocurarine have higher affinity in BK than in Kv1.3 was confirmed in electrophysiological experiments with the intracellular application of the ligand (Figs. 7 and 8).

According to calculations, residues that provide the largest

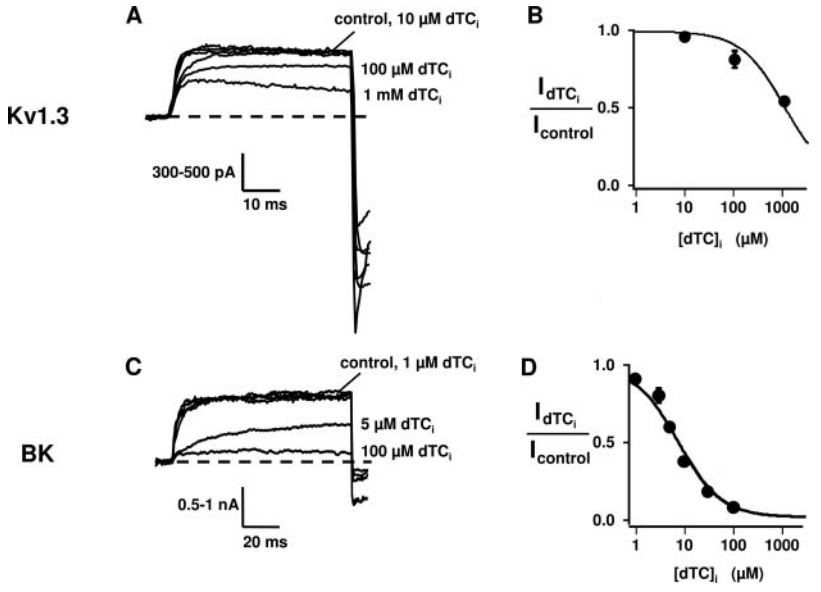

Fig. 8. Whole cell patch-clamp experiment on L929 or CHO-K1 cells permanently transfected with mKv1.3 (top row) and BK channels (bottom row), respectively. A, currents through mKv1.3 channels were elicited by stepping the voltage to +40 mV for 50 ms from a holding potential of −80 mV every 30 s. The bath solution contained 164.5 mM K^+. Currents from three independent experiments are shown. Currents without dTC_i (control) were obtained in each experiment right after break-in (<1 min) and used to normalize the current. The current with the different dTC_i concentrations were obtained after at least 15 min of break-in. B, dose-response curve for dTC_i to block current through Kv1.3 channels. The K_d value (1 ± 0.3 mM) for dTC_i block was deduced by fitting a modified Hill equation ($I_{dTCi}/I_{control} = 1/[1 + ([dTC_i]/K_d)]$) to the data points, where I_{dTCi} is the peak current in the presence of dTC_i (>15 min after break-in) and $I_{control}$ is the peak current in the apparent absence of dTC_i (<1 min after break-in). The value at each dTC_i concentration was the mean ± S.D. of two to four measurements. SD is shown as bars when it exceeds the size of the symbol. C, currents through BK channels were elicited by stepping the voltage to +100 mV for 100 ms from a holding potential of −80 mV every 30 s. The bath solution contained 164.5 mM K^+. Currents from four independent experiments are shown. Currents without dTC_i (control) were obtained in each experiment right after break-in and used to normalize the current. The current with the different dTC_i concentrations were obtained after at least 15 min of break-in. D, dose-response curve for the dTC_i to block current through BK channels. The K_d value (7.64 ± 0.014 μM) for the dTC_i block was deduced similarly as described in B. The value at each dTC_i concentration was the mean ± S.D. of two to five measurements.

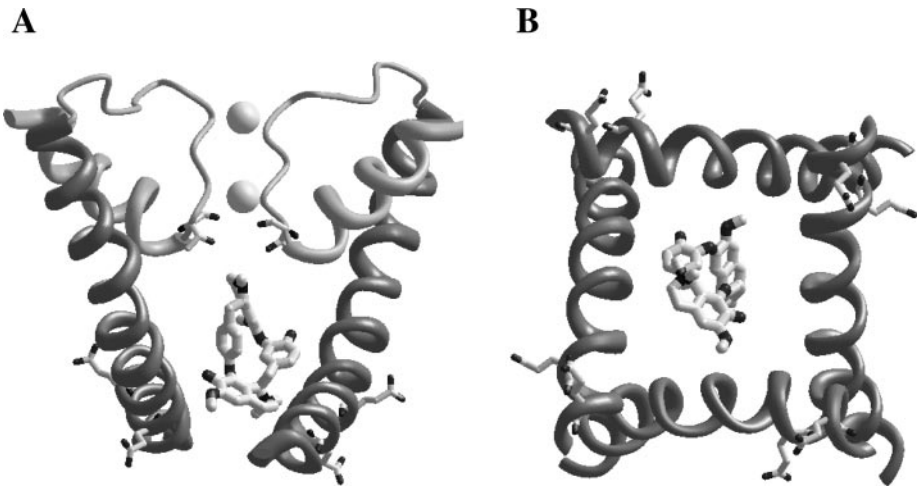

Fig. 9. Side (A) and cytoplasmic (B) views of the lowest energy complex *d*-tubocurarine-BK with Glu^{i24} and Glu^{i27} shown as sticks protruding from the inner helices.

stabilizing contributions to the binding energy of *d*-tubocurarine are in positions p48 and p49 at the cytoplasmic side of the selectivity filter region as well as in the pore-facing positions i15, i18, i19, and i22 of the inner helices (Tables 1, 3, and 4). Structurally different drugs are known to bind in the inner pore of different K^+ channels. Recent mutational and ligand-binding experiments (Mitcheson et al., 2000; Hanner at al. 2001; Seebohm et al., 2003; Decher et al., 2004) revealed patterns of residues in the inner helixes and P-loops that interact with ligands (Table 1). Positions of *d*-tubocurarine-sensing residues predicted in our study are in a good agreement with these patterns (Table 1).

A common feature of the lowest energy complexes of *d*-tubocurarine in BK and Kv1.3 is binding of the protonated amino group below the selectivity filter region, at the K^+ dehydration site. The complexes are stabilized by favorable electrostatic interactions of the ligand's cationic group with Thr^{p49} and Ser^{p48}/Thr^{p48} as well as with macrodipoles of the pore helices. Not surprisingly, the ligand-receptor interactions are highly sensitive to the population of K^+ binding sites in the selectivity filter region, being destabilized by K^+ in position 4 (Table 2). Increasing evidence suggest that C-type inactivation is associated with the altered population of the K^+ binding sites (Zhorov and Tikhonov, 2004; Berneche and Roux, 2005; Lenaeus et al., 2005). Further experimental and theoretical studies are necessary to explain the intriguing observations that both cationic drugs such as *d*-tubocurarine and nucleophilic ligands such as correolide, which lacks cationic groups, exhibit high affinity in the C-type inactivated K^+ channels.

According to calculations, electrostatic ligand-receptor interactions in Kv1.3 are weaker than in BK. It should be noted, however, that electrostatic interactions are highly sensitive to the model setup, being the least reliable component of the ligand-receptor energy. Therefore, the cause(s) of the low affinity of *d*-tubocurarine to the open Kv1.3 remain to be elucidated in future experiments and computations. In particular, a higher affinity of *d*-tubocurarine in BK versus Kv1.3 may be caused by the rings of negatively charged residues Glu^{i24} and Glu^{i27} at the entrance to the internal vestibule (Table 1). It is noteworthy that the Glu^{i24} residues are approximately at the level of the ammonium group of *d*-tubocurarine bound in BK, but they face away from the pore axis and do not form direct contacts with the ligand (Fig. 9). Although the acidic residues do not face the permeation pathway, they contribute to the large conductance of BK channels and prevent inward rectification by increasing the concentration of potassium ions in the vestibule (Brelidze et al., 2003). The mutation Ala^{i23}Asp increased KcsA conductance in a pH-dependent manner (Nimigean et al., 2003). Further studies are necessary to explore whether negatively charged residues at the cytoplasmic side of the pore augment affinity of dicationic drug.

In conclusion, in this work we proposed the binding modes of *d*-tubocurarine in K^+ channels and predicted that the energy of *d*-tubocurarine in BK is more preferable than in Kv1.3. Subsequent experiments demonstrated that the internally applied *d*-tubocurarine has a higher affinity in BK than to Kv1.3, suggesting that the X-ray structure of MthK, which was used to model BK, remains the best available template to model Ca^{2+}- and ligand-activated P-loop channels. Bulky semirigid drugs are sensitive probes to explore architecture of the inner pore in P-loop channels. The repertoire of such ligands is large, and interesting structure-activity relationships have been reported (Felix et al., 1992). Interpretation of such observations with molecular modeling can help to map receptors for medically important drugs.

Acknowledgments

We thank Iva Bruhova for reading the manuscript and for valuable comments. Computations were performed, in part, using the SHARCNET Supercomputer Centre (McMaster University).

References

Baron A, Frieden M, Chabaud F, and Beny JL (1996) Ca^{2+}-dependent non-selective cation and potassium channels activated by bradykinin in pig coronary artery endothelial cells. *J Physiol (Lond)* **493:**691–706.

Berneche S and Roux B (2005) A gate in the selectivity filter of potassium channels. *Structure* **13:**591–600.

Birnbaum SG, Varga AW, Yuan LL, Anderson AE, Sweatt JD, and Schrader LA (2004) Structure and function of Kv4-family transient potassium channels. *Physiol Rev* **84:**803–833.

Brelidze TI, Niu X, and Magleby KL (2003) A ring of eight conserved negatively charged amino acids doubles the conductance of BK channels and prevents inward rectification. *Proc Natl Acad Sci USA* **100:**9017–9022.

Brooks CL, Pettitt BM, and Karplus M (1985) Structural and energetic effects of truncating long ranged interactions in ionic polar fluids. *J Chem Phys* **83:**5897–5908.

Bruhova I and Zhorov BS (2005) KvAP-based model of the pore region of Shaker potassium channel is consistent with cadmium- and ligand-binding experiments. *Biophys J* **89:**1020–1029.

Chandy KG, Wulff H, Beeton C, Pennington M, Gutman GA, and Cahalan MD (2004) K^+ channels as targets for specific immunomodulation. *Trends Pharmacol Sci* **25:**280–289.

Codding PW and James MNG (1973) The crystal and molecular structure of a potent neuromuscular blocking agent: d-tubocurarine dichloride pentahydrate. *Acta Crystallogr B* **29:**935–942.
Decher N, Pirard B, Bundis F, Peukert S, Baringhaus KH, Busch AE, Steinmeyer K, and Sanguinetti MC (2004) Molecular basis for Kv1.5 channel block: conservation of drug binding sites among voltage-gated K^+ channels. *J Biol Chem* **279:**394–400.
Dewar MJS, Zoebisch EG, Healy EF, and Stewart JJP (1985) AM1: a new general purpose quantum mechanical molecular model. *J Am Chem Soc* **107:**3902–3909.
Doyle DA, Morais Cabral J, Pfuetzner RA, Kuo A, Gulbis JM, Cohen SL, Chait BT, and MacKinnon R (1998) The structure of the potassium channel: molecular basis of K^+ conduction and selectivity. *Science (Wash DC)* **280:**69–77.
Egan TM, Dagan D, and Levitan IB (1993) Properties and modulation of a calcium-activated potassium channel in rat olfactory bulb neurons. *J Neurophysiol* **69:**1433–1442.
Felix JP, King VF, Shevell JL, Garcia ML, Kaczorowski GJ, Bick IR, and Slaughter RS (1992) Bis(benzylisoquinoline) analogs of tetrandrine block L-type calcium channels: evidence for interaction at the diltiazem-binding site. *Biochemistry* **31:**11793–11800.
Go N and Scheraga HA (1970) Ring closure and local conformational deformations of chain molecules. *Macromolecules* **3:**178–187.
Grissmer S, Nguyen AN, Aiyar J, Hanson DC, Mather RJ, Gutman GA, Karmilowicz MJ, Auperin DD, and Chandy KG (1994) Pharmacological characterization of five cloned voltage-gated K^+ channels, types Kv1.1, 1.2, 1.3, 1.5 and 3.1, stably expressed in mammalian cell lines. *Mol Pharmacol* **45:**1227–1234.
Hamill OP, Marty A, Neher E, Sakmann B, and Sigworth FJ (1981) Improved patch-clamp techniques for high resolution current recording from cells and cell-free membrane patches. *Pflueg Arch Eur J Physiol* **391:**85–100.
Hanner M, Green B, Gao YD, Schmalhofer WA, Matyskiela M, Durand DJ, Felix JP, Linde AR, Bordallo C, Kaczorowski GJ, et al. (2001) Binding of correolide to the K(v)1.3 potassium channel: characterization of the binding domain by site-directed mutagenesis. *Biochemistry* **40:**11687–11697.
Hanner M, Schmalhofer WA, Green B, Bordallo C, Liu J, Slaughter RS, Kaczorowski GJ, and Garcia ML (1999) Binding of correolide to K(v)1 family potassium channels. Mapping the domains of high affinity interaction. *J Biol Chem* **274:**25237–25244.
Hille B (2001) *Ionic Channels of Excitable Membrane*, Sinauer Associates, Inc., Sunderland, MA.
Jiang Y, Lee A, Chen J, Cadene M, Chait BT, and MacKinnon R (2002) Crystal structure and mechanism of a calcium-gated potassium channel. *Nature (Lond)* **417:**515–522.
Jiang Y, Lee A, Chen J, Ruta V, Cadene M, Chait BT, and MacKinnon R (2003) X-ray structure of a voltage-dependent K^+ channel. *Nature (Lond)* **423:**33–41.
Kuo A, Gulbis JM, Antcliff JF, Rahman T, Lowe ED, Zimmer J, Cuthbertson J, Ashcroft FM, Ezaki T, and Doyle DA (2003) Crystal structure of the potassium channel KirBac1.1 in the closed state. *Science (Wash DC)* **300:**1922–1926.
Lazaridis T and Karplus M (1999) Effective energy function for proteins in solution. *Proteins Struct Funct Genet* **35:**133–152.
Lenaeus MJ, Vamvouka M, Focia PJ, and Gross A (2005) Structural basis of TEA blockade in a model potassium channel. *Nat Struct Mol Biol* **12:**454–459.
Li Z and Scheraga HA (1987) Monte Carlo-minimization approach to the multiple-minima problem in protein folding. *Proc Natl Acad Sci USA* **84:**6611–6615.
Long SB, Campbell EB, and MacKinnon R (2005a) Crystal structure of a Mammalian voltage-dependent shaker family K^+ channel. *Science (Wash DC)* **309:**897–903.
Long SB, Campbell EB, and Mackinnon R (2005b) Voltage sensor of Kv1.2: structural basis of electromechanical coupling. *Science (Wash DC)* **309:**903–908.
Mathie A, Wooltorton JR, and Watkins CS (1998) Voltage-activated potassium channels in mammalian neurons and their block by novel pharmacological agents. *Gen Pharmacol* **30:**13–24.
Mitcheson JS, Chen J, Lin M, Culberson C, and Sanguinetti MC (2000) A structural basis for drug-induced long QT syndrome. *Proc Natl Acad Sci USA* **97:**12329–12333.
Nimigean CM, Chappie JS, and Miller C (2003) Electrostatic tuning of ion conductance in potassium channels. *Biochemistry* **42:**9263–9268.
Rauer H and Grissmer S (1996) Evidence for an internal phenylalkylamine action on the voltage-gated potassium channel Kv1.3. *Mol Pharmacol* **50:**1625–1634.
Reynolds CD and Palmer RA (1976) The crystal structure, absolute configuration and stereochemistry of (+)-tubocurarine dibromide methanol solvate: a potent neuromuscular blocking agent. *Acta Crystallogr B* **32:**1431–1439.
Seebohm G, Chen J, Strutz N, Culberson C, Lerche C, and Sanguinetti MC (2003) Molecular determinants of KCNQ1 channel block by a benzodiazepine. *Mol Pharmacol* **64:**70–77.
Tamargo J, Caballero R, Gomez R, Valenzuela C, and Delpon E (2004) Pharmacology of cardiac potassium channels. *Cardiovasc Res* **62:**9–33.
Tikhonov DB and Zhorov BS (1998) Kinked-helices model of the nicotinic acetylcholine receptor ion channel and its complexes with blockers: simulation by the Monte Carlo minimization method. *Biophys J* **74:**242–255.
Tikhonov DB and Zhorov BS (2005) Modeling p-loops domain of sodium channel: homology with potassium channels and interaction with ligands. *Biophys J* **88:**1–14.
Webster SM, Camino D, Dekker JP, and Yellen G (2004) Intracellular gate opening in Shaker K^+ channels defined by high-affinity metal bridges. *Nature (Lond)* **428:**864–868.
Weiner J, Kollman PA, Case DA, Singh UC, Chio C, Alagona G, Profeta S, and Weiner PK (1984) A new force field for molecular mechanical simulation of nucleic acids and proteins. *J Am Chem Soc* **106:**765–784.
Yellen G (2001) Keeping K^+ completely comfortable. *Nat Struct Biol* **8:**1011–1013.
Zhorov BS and Brovtsyna NB (1993) Conformational analysis of d-tubocurarine: implications for minimal dimensions of its binding site within ion channels. *J Membr Biol* **135:**19–26.
Zhorov BS, Brovtsyna NB, Gmiro VE, Lukomskaya N, Serdyuk SE, Potapyeva NN, Magazanik LG, Kurenniy DE, and Skok VI (1991) Dimensions of the ion channel in neuronal nicotinic acetylcholine receptor as estimated from analysis of conformation-activity relationships of open-channel blocking drugs. *J Membr Biol* **121:**119–132.
Zhorov BS and Tikhonov DB (2004) Potassium, sodium, calcium and glutamate-gated channels: pore architecture and ligand action. *J Neurochem* **88:**782–799.
Zhou X-B, Schlossmann J, Hofmann F, Ruth P, and Korth M (1998) Regulation of stably expressed and native BK channels from human myometrium by cGMP- and cAMP-dependent protein kinase. *Pflueg Arch Eur J Physiol* **436:**725–734.
Zhou Y and MacKinnon R (2003) The occupancy of ions in the K^+ selectivity filter: charge balance and coupling of ion binding to a protein conformational changes underlie high conduction rate. *J Mol Biol* **333:**965–975.
Zhou Y, Morais Cabral JH, Kaufman A, and MacKinnon R (2001b) Chemistry of ion coordination and hydration revealed by K^+ channel-Fab complex at 2 A resolution. *Nature (Lond)* **414:**43–48.
Zhou Y, Morais Cabral JH, Mann S, and MacKinnon R (2001a) Potassium channel receptor site for the inactivation gate and quaternary amine inhibitors. *Nature (Lond)* **411:**657–661.

Address correspondence to: Dr. Boris S. Zhorov, Department of Biochemistry and Biomedical Sciences, McMaster University, 1200 Main St. West, Hamilton, ON L8N 3Z5, Canada. E-mail: zhorov@mcmaster.ca